IV Journeys in Multiphase Flows (JEM 2017)
March 27-31, 2017, São Paulo, SP, Brazil

Paper ID: JEM-2017-0048

# EFFECTS OF CHANNEL INCLINATION ON TWO-PHASE FLOW CHARACTERISTICS FOR SMALL DIAMETER CHANNELS

**Francisco Loyola Lavin**
Department of Mechanical Engineering, University of Magallanes, Avenida Bulnes 01855, Punta Arenas, Chile.
francisco.loyola@umag.cl, francisco.loyola@usp.br

**Fabio Toshio Kanizawa**
Laboratory of Thermal Sciences (LATERMO), Department of Mechanical Engineering (TEM/PGMEC), Universidade Federal Fluminense (UFF). Rua Passo da Pátria, 156, 302-D, Niterói, Rio de Janeiro, Brazil. CEP 24210-240.
fabio.kanizawa@mec.uff.br

**Gherhardt Ribatski**
Heat Transfer Research Group, Department of Mechanical Engineering, Escola de Engenharia de (EESC), University of São Paulo. Av. Trabalhador São Carlense, 400, São Carlos, São Paulo, Brazil.
ribatski@sc.usp.br

***Abstract.*** *An experimental investigation was carried out to elucidate the effect of the channel inclination on two-phase flow characteristics. Air/water flow was investigated inside a rectangular channel, 6.0 mm deep and 6.5 mm wide. The channel inclination varied from -90º to +90° relative to the horizontal plane. Flow patterns were identified and pressure drop was measured for mass velocities between 90 and 760 kg/m²s, corresponding to gas and liquid superficial velocities ranging from 0.09 to 19.4 m/s, and from 0.1 to 0.76 m/s, respectively. Flow patterns maps were developed according to the following approaches: (i) subjective approach based on flow images captured through a high-speed video camera; (ii) objective approach based a data-grouping algorithm, using metrics based on signals from the two-phase flow. Three flow patterns were identified: bubble, intermittent and annular. Stratified flows were not observed. Major differences in flow patterns transitions are observed comparing upward and downward flow. In general, the total pressure drop increased with increasing channel inclination, due to the contribution of the gravitational pressure drop parcel. In this study, the frictional pressure drop was estimated from the total pressure drop using different void fraction methods to estimate the gravitational parcel during inclined flow.*

***Keywords:*** *Two-phase flow; Pressure Drop; Flow pattern; Void fraction; Inclined channel.*

## 1. INTRODUCTION

Heat exchangers based on small diameter channels present several advantages when compared with those based on conventional channels. As pointed out by Ribatski *et al*. (2007), the heat transfer coefficient increases with decreasing channel diameter. Moreover, the ratio between the effective heat transfer area and the volume of the heat exchanger increases with tube diameter reduction, and small channels allow operation under higher pressures due to their higher robustness. However, the pressure drop increases with decreasing channel size, which impacts the pumping power and overall system efficiency, which requires an optimum design of the heat exchanger. Therefore, an accurate understanding of two-phase flow and pressure drop mechanisms is needed in order of making two-phase flow cooling feasible for applications in industrial sectors such as automotive and avionics, air-conditioning, electronics cooling and high performance computers as indicated by Kim and Mudawar (2014), Coleman and Garimella (2003) and Do Nascimento and Ribatski (2010).

Few studies in literature are devoted to the investigation of the effects of flow inclination on the two-phase flow patterns and pressure drop in reduced diameter channels. Considering the case of channels with dimensions close to the transition between micro and conventional channels, which is the focus of the present study, the number of studies available in the open literature is even smaller. Experimental results for flow pattern under geometrical and fluid conditions similar to the present study were obtained by Coleman and Garimella (1999), Wölk *et al*. (2000) and Chen *et al*. (2009). Zhao *et al*. (2004) also investigated the impact of channel inclination on two-phase flow parameters, but the authors used a smaller channel in their experimental campaign. Wambsganss *et al*. (1992), Lee and Lee (2001) performed pressure drop measurements for air-water flows in horizontal rectangular channels. Mishima *et al*. (1993), Mishima and Hibiki (1996) and Ide *et al*. (2007) investigated frictional pressure drop and void fraction for upward air-water flows in channels with dimensions approximately similar to the present study.

In this scenario, it is important to elucidate the influence of gravitational effects on two-phase distribution during gas-liquid flows in channels with dimensions close to the transition between micro and macro-scale, because the channel inclination affects the distribution of phases and their real velocities. In this context, the present study reports experimental results on pressure drop and flow patterns characteristics for air-water flows inside a rectangular channel with cross-section of 6.0 x 6.5 mm². The experimental database comprises data for mass velocities ranging from 90 to 760 kg/m²s, corresponding to gas and liquid superficial velocities ranging from 0.09 to 19.4 m/s and from 0.1 to 0.76 m/s, respectively. Results were obtained for channel inclinations ranging from -90° to +90° relative to the horizontal plane. Flow patterns were identified based on subjective and objective approaches. The subjective classification was performed with the help of flow images captured with a high speed video camera, and the objective classification was based on the k-means clustering method using transient pressure drop and optical signals.

## 2. EXPERIMENTAL APPARATUS AND PROCEDURE

The experimental facility consists of a main circuit, a water closed loop, compressed air conditioning and injection systems, and a temperature control circuit. The working fluids are air and deionized water with temperature close to laboratory room and close to the atmospheric pressure. The main circuit is schematically depicted in Figure 1, and comprises the water loop, the air conditioning section and the test section.

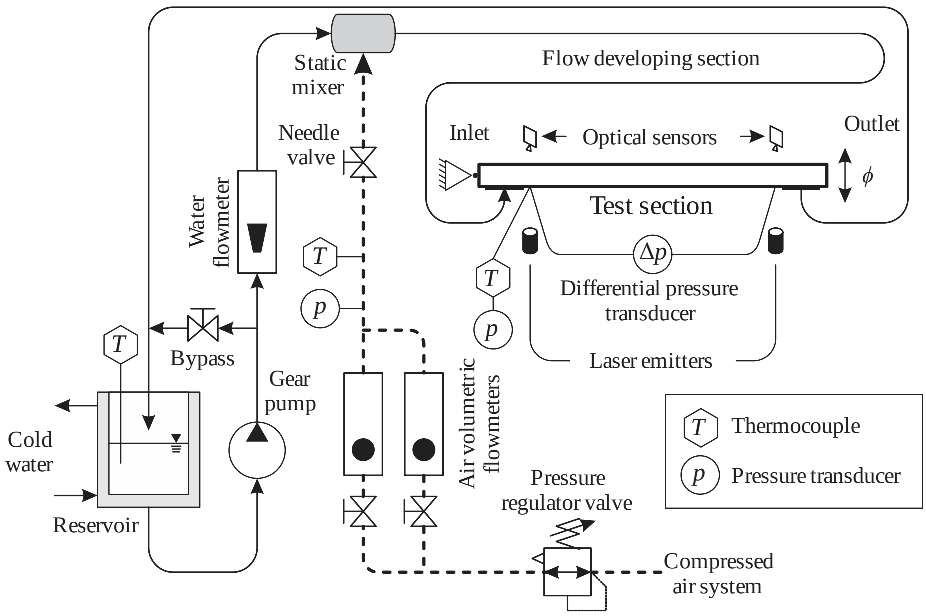


Figure 1. Schematics of the main experimental circuit.

In the main circuit, water is driven from the reservoir by a gear pump, powered by a variable-frequency inverter actuated by the data acquisition and control system. The volumetric water flow rate is measured with a rotameter with measuring range between 96 and 1881 ml/min, and uncertainty of ±5% of its set span. This rotameter allows determination of water superficial velocities between 0.04 and 0.80 m/s with a maximum uncertainty of ±0.02 m/s. The water is stored and has its temperature controlled in a jacketed reservoir, where water from a small chiller flows in the jacket side of the tank, keeping the temperature of the liquid in the test loop at 20 ± 1 °C.

The air is supplied by a compressed air line available in the laboratory. The compressed air firstly passes through a filter-dryer and a pressure regulator valve. Downstream this valve, the volumetric flow rate of air is determined with a measuring system composed by two rotameters with embodied needle valves used to set the flow rate. The rotameters measure air flow rates from 0.04 to 0.5 l/min and 0.4 to 5 l/min for air, which is equivalent to superficial velocities ranging from 0.07 to 20 m/s, with uncertainty of ±0.1 m/s. The database of the present study contains only 4.8% of data with superficial gas velocity in the range 0.09 – 0.12 m/s, which corresponds to the conditions with the highest relative error. During the experiments, only one rotameter is used by closing the needle valve of the other rotameter; and the active rotameter is selected based on the desired superficial velocity. An absolute pressure transducer and a thermocouple are installed just downstream the flowmeters with the objective of determining the air thermodynamic state. Hence, based on the local density and volumetric flow rate of the air, it is possible to evaluate its mass flow rate. And based on the measurements of pressure and temperature in the test section, and from the continuity, it is possible to evaluate the gas superficial velocity in the test section. Finally, the air is radially directed in the two-phase static mixer, as schematically illustrated in Figure 2.

The static mixer is composed of a porous media, and was designed and selected to avoid possible intermittence in the flow rate, and is depicted in Figure 2. The porous media is made of sintered silicon carbide and provides dispersed air bubbles with diameter between 100-500 μm. The water flow through the internal channel of the porous media with 5 mm in diameter and 35 mm long, and the external mixer surface of the mixer is exposed to the compressed air.

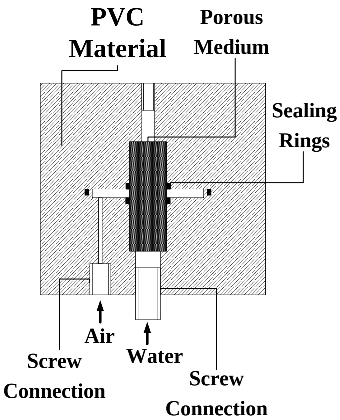


Figure 2. Schematics of the two-phase static mixer.

The test section consists of a rectangular channel made of superposed acrylic plates, with the channel cross section 6.5 mm wide, 6.0 mm high and 1,200 mm long, measured between the inlet and outlet connections. A fast response differential pressure transducer model Validyne DP15 with accuracy of ±0.5% and the diaphragm 30 (measuring range between 0 and 8.6 kPa) was used for the pressure drop measurement, and its taps were connected to drilled holes with 2 mm in diameter, which are 180 mm distant from the inlet and outlet sections. Care was exercised in order of keeping only liquid in the tubes connecting the both sides of the diaphragm and the test section.

A high speed video camera model Optronis CAMRECORD 600 was used to capture the flow images with a recording rate of 1000 frames/s and a resolution of 1280 pixels x 512 pixels. Two pairs of laser emitters and sensors apart from 180 mm away from the inlet and outlet sections were used to investigate the flow pattern characteristics, as schematically depicted in Figure 1, because the light intensity detected by the laser sensors varies with the two-phase flow topology.

The experimental procedure was initiated first by setting the inclination angle of the test section and the water temperature in the reservoir equal to 20 °C. After this initial procedure, water flow was imposed by actuating in the gear pump. Then, all the transducers were checked for water single-phase flow to verify any possible incoherence in their measurements. Then, the air was circulated and its flow rate adjusted by manipulating the needle valves of the flow meters. Steady state conditions were assumed and the data recorded when variations in the flow rate indicated by the rotameters become imperceptible. Flow images and the signal from the transducers were simultaneously recorded with an acquisition rate of 1000 data points/second for a period of 1 minute.

The subjective approaches for flow patterns identification was based on analysis of images and/or videos. The flow patterns dispersed bubbles, intermittent and annular flow were classified according to definitions presented by Cheng *et al*. (2008). Analogous to Su and Dy (2004) and Sempértegui-Tapia *et al*. (2013), the flow patterns were also characterized objectively using the k-means clustering method based on the following metrics: (i) the standard deviation of the pressure drop signal; (ii) the ratio between the standard deviation and the mean value of the pressure drop signal and; (iii) the ratio between the standard deviation and the mean value of the transient signal of the laser sensor located close to the outlet of the test section.

The frictional pressure drop parcel was obtained from the measured total pressure drop as follows:

$$\Delta p_f = \Delta p_{total} - \Delta p_g - \Delta p_a \tag{1}$$

where $\Delta p_{total}$ is the total pressure drop determined from the differential pressure transducer, and is composed by the gravitational $\Delta p_g$, accelerational $\Delta p_a$ and frictional parcels $\Delta p_f$. The total pressure drop is given by the differential pressure transducer discounting the contribution of the liquid column due to fluid inside the capillary tubes connecting the terminals of the pressure transducer to the test section taps. Accelerational pressure drop parcel was assumed as negligible. The gravitational parcel depends of the channel inclination $\phi$, distance between pressure taps $L$, and the superficial void fraction α along the channel as follows:

$$\Delta p_g = [(1-\alpha)\rho_l + \alpha\rho_g]gL\sin\phi \tag{2}$$

It can be noted that the estimative of void fraction is necessary to the evaluation of $\Delta p_g$. Therefore, a correct estimative of the frictional pressure drop parcel depends on the accuracy of the void fraction predictive method.

## 3. EXPERIMENTAL RESULTS

In the present, study more than 2,000 experimental data were obtained for inclination angles relative to the horizontal plane, as described in Tab.1.

Table 1. Database description.

| Inclination angle, $\phi$ [°] | Number of data points |
|---|---|
| Horizontal, 0 | 342 |
| Upward, 30 | 298 |
| Upward, 60 | 308 |
| Upward, 90 | 292 |
| Downward, -90 | 299 |
| Downward, -60 | 299 |
| Downward, -30 | 286 |
| Total | 2,124 |

### 3.1 Flow patterns

Figure 3 depicts the flow pattern results for different channel inclinations $\phi$. In this figure, the symbols correspond to the flow patterns identified subjectively, and the dotted lines correspond to the transitions identified based on the k-means method.

Three flow patterns are identified in Figure 3 according to the classification presented by Cheng et al. (2008): bubbles, intermittent and annular. Flow images were included in the plots to illustrate the local flow patterns, and highlight the influence of gravity as the channel inclination varies. It can be noticed that subjective and objective approaches provide similar trends and transition lines.

Based on the flow pattern results, it is notorious the wider region corresponding to bubble flow for $\phi$ of 0 and 30º, compared with other channel inclinations. As pointed out by Barnea and Taitel (1986) for conventional channels, intermediate inclination angles favor the concentration of dispersed bubbles in the upper region of the channel, which combined with the different bubble velocities caused by buoyancy forces in the flow direction, promotes an earlier transition to intermittent flow. On the other hand, for conditions of horizontal and near horizontal channels, this effect is suppressed and the transition to intermittent flow is delayed, and the bubbles flow pattern is observed for a wider range of operational conditions, as shown in Figure 3.

It can be also noted in Figure 3 that for downward flow (vertical and inclined) the region corresponding to annular flow becomes wider. This behavior is related to the fact that the liquid tends to flow as a film on the channel surface for downwards flow even for reduced flow velocities, similar to the condition of falling film.

The bubbles shape for vertical upward and downward flows are distinct, as can be observed based on the flow images depicted in Figure 3. For downward flows, under conditions of low and intermediate superficial velocities, the bubbles nose is flat, on contrary to downward flow for which the bubbles front presents a bullet shape.

Figure 4 illustrates the effect of the flow inclination angle on the flow patterns transitions characterized based on the objective method for vertical and inclined, upward and downward flows. According to this figure, it can be concluded that no significant difference is observed in the flow pattern transitions for horizontal and upward vertical and inclined flows. Hence, it can be speculated that the dominant mechanisms related to flow pattern transitions during horizontal and upward flows are similar. On the other hand, for condition of downward flow a significant difference is observed mainly for the transition between intermittent and annular flows when compared with horizontal flows. This difference can be attributed to the gravitational effects that induces a higher liquid velocity. Finally, according to Figure 4 the major differences between flow pattern transitions for upward and downward flow is observed for the following conditions: (i) transition from intermittent to annular flow pattern; (ii) low liquid superficial velocities.

For the conditions evaluated in the present study, it is worth mentioning that stratified flows were not observed, and this aspect is related to the fact that the channel dimension is close to the transition between micro and conventional scales according to the Kew and Cornwell (1997) methodology; and for micro scale channel the gravitational effects have reduced contribution.

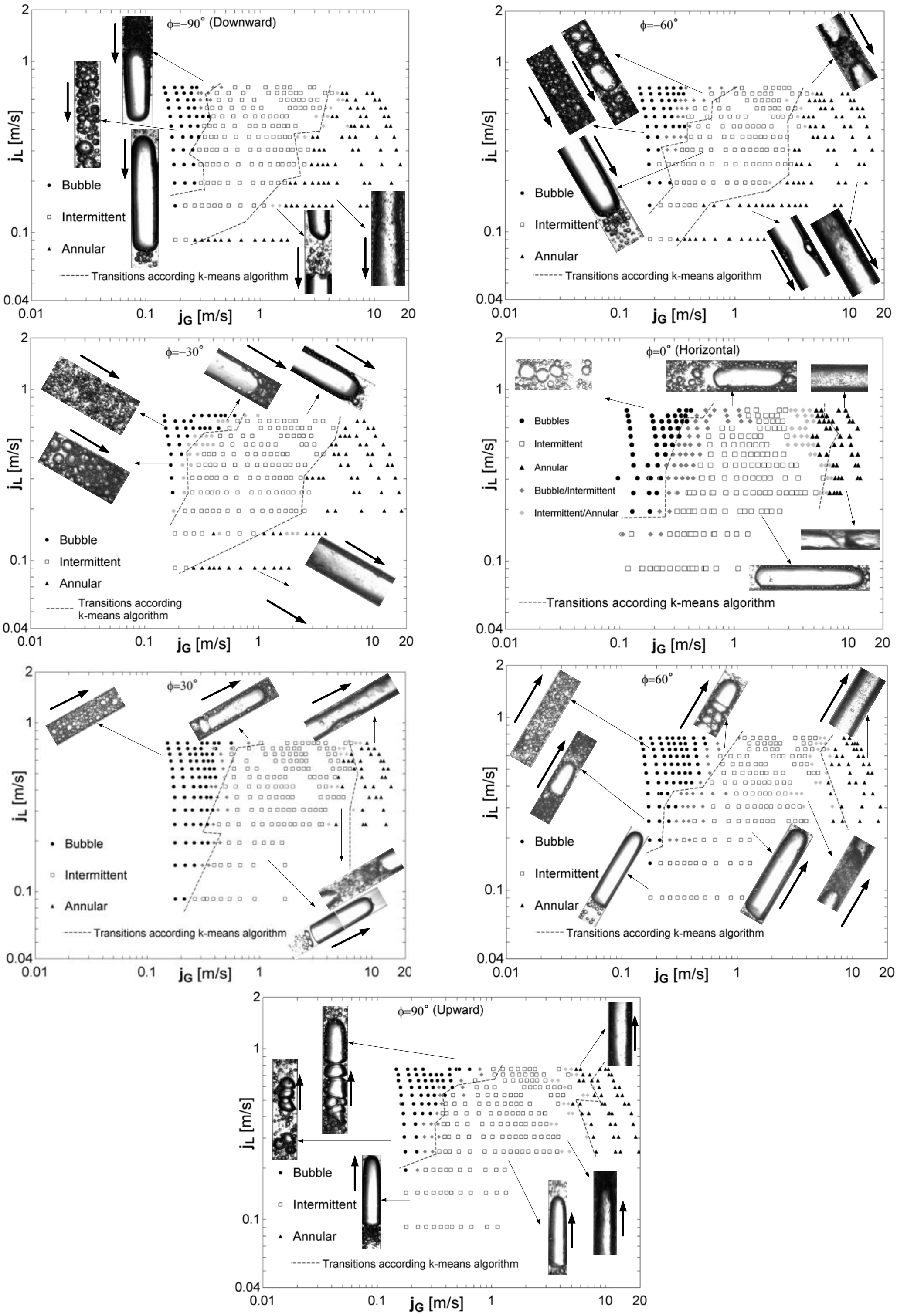


Figure 3. Flow pattern results for different channel inclinations $\phi$, based on subjective (symbols) and objective (dotted lines) methods.

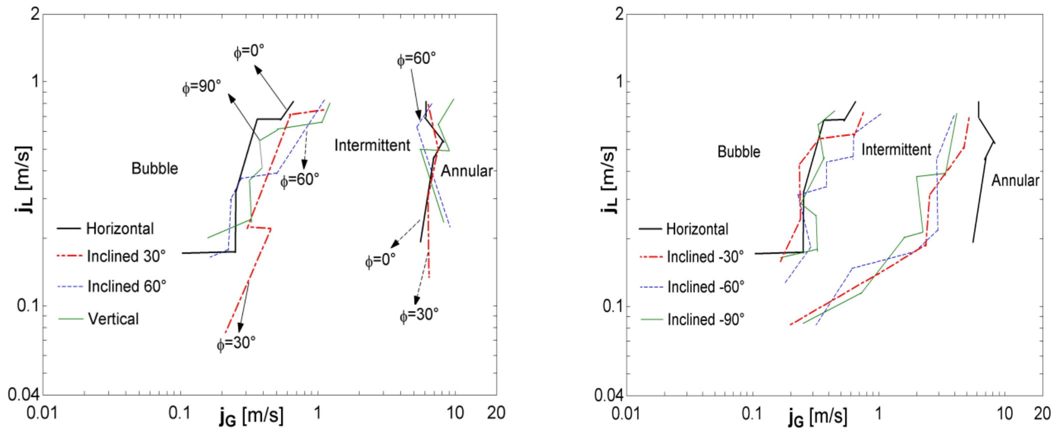


Figure 4. Illustration of the effect of the inclination angle ϕ on the Flow pattern transitions based on the k-means method for (a) upward and (b) downward flows.

## 3.2 Pressure drop

Initially, single-phase flow experiments were performed for different inclination angles with the objective of validating the experimental facility and the data regression procedure. Figure 5 presents a comparison of the experimental data and the corresponding predictions for frictional pressure drop. According to this figure, the experimental data and the predictions agree reasonably well with 71.4 and 93.4 % of the experimental results correctly predicted within error margins of ±20 and 30%, respectively. In this comparison, the pressure drop for laminar flow was estimated according to the correlation of Shah and London (1978). For transitional and turbulent flow regimes, corresponding to Reynolds numbers higher than 2,300, the friction factor was estimated according to Blasius correlation for round channels using the hydraulic diameter as the characteristic length. Based on this analysis, it can be concluded that the experimental facility and regression procedure are capable of providing reliable pressure drop measurements for single and two-phase flow experiments.

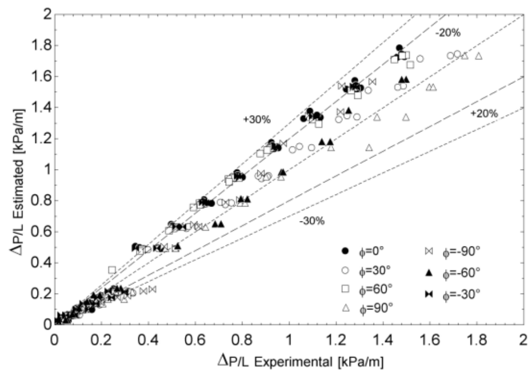


Figure 5. Comparison of data predicted according to well established method from literature for frictional pressure drop and experimental results for liquid single-phase flow.

Figure 6 depicts the effect on the frictional pressure drop of varying the superficial gas velocity for a fixed superficial liquid velocity for horizontal two-phase flow. According to this figure, for $j_L$= 0.419 m/s at the transition between bubble and intermittent flow patterns, the frictional pressure drop gradient presents a local peak at intermediate $j_G$ values. This result emphasize the importance of correct and reliable flow patterns predictive method, which also impacts in the two-phase parameters such as pressure drop and heat transfer coefficient.

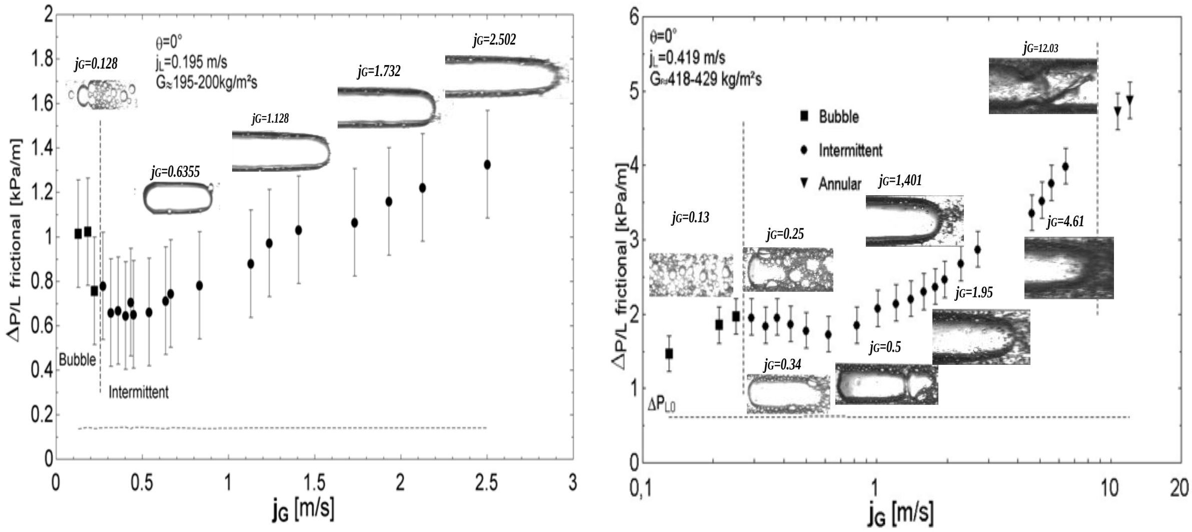


Figure 6. Variation of the frictional pressure drop with $j_G$ under conditions of fixed $j_L$ for horizontal flow. The flow patterns were objectively characterized.

Figure 7 illustrates the variation of the total and frictional parcel of pressure drop with $j_G$ for horizontal and upward flow for inclined channels. As above-mentioned, the prediction of the void fraction affects the evaluation of $\Delta p_g$, and, consequently, $\Delta p_f$ . Based on this figure, it can be noticed that $\Delta p_{total}$ increases with increasing the channel inclination for upward flow due to the contribution of the gravitational pressure drop parcel. This influence becomes more pronounced for reduced values of $j_L$ and $j_G$, since for these conditions the contribution of $\Delta p_g$ on $\Delta p_{total}$ is higher. For inclined channels ($\phi$ > 0°) the total pressure drop diminishes with the increment of $j_G$. This behavior results from the fact that the superficial void fraction increases with increasing the superficial gas velocity implying on the reduction of $\Delta p_g$, and, and consequently of $\Delta p_{total}$.

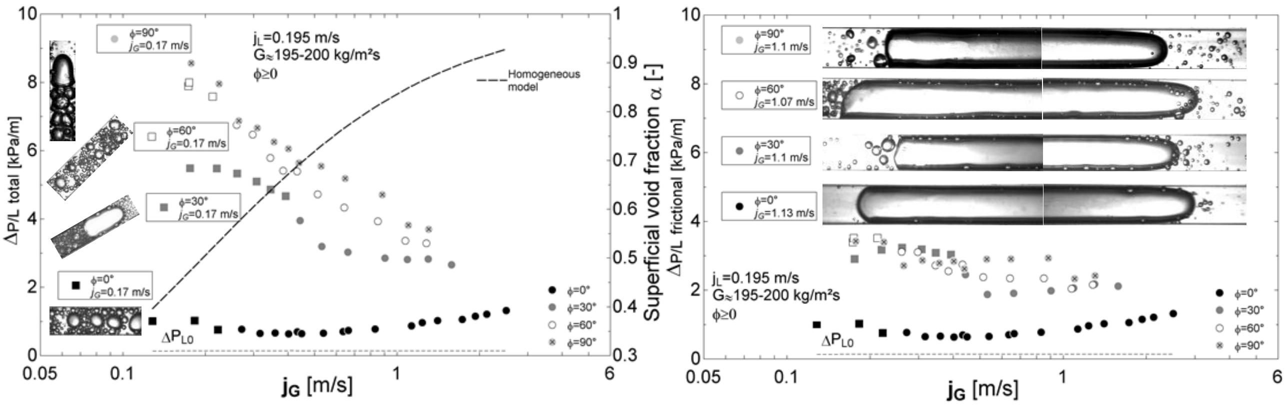


Figure 7. Variation of $\Delta p_{total} / L$ and $\Delta p_f / L$ with $j_G$ for distinct channel inclinations ($\phi \geq 0°$). Void fraction is evaluated according to the homogeneous model.

Using the two pairs of laser emitter-sensor, an evaluation of the gas bubbles velocity was made analogously that of Sempértegui-Tapia *et al*. (2013). In this analysis it is considered that the cross section is intermittently occupied by liquid and gas phases. The experimental results for this analysis presented high void fraction values, being even higher than those predicted by the homogeneous model, and this aspect is mainly attributed to the gas expansion due to the pressure drop between the sensors, and to the liquid film present during the gas bubbles passage that could not be considered in the method due to the absence of measurement method for this parameter. Nonetheless, it can be concluded that the void fraction value are relatively high for the experimental conditions in the present study, hence the homogeneous void fraction is adopted in this study. With these considerations, Fig. 7 also depicts the effect of $j_G$ on the frictional pressure drop which value was estimated based on the total pressure drop using to the homogeneous model to estimate the void fraction, given by Eq. (1).

According to Figure 7, the frictional pressure drop parcel is higher for upward vertical and inclined flows when compared to horizontal flow for similar experimental conditions. This difference can be attributed to the difference in flow characteristics, and to the agreement between the homogeneous void fraction model and the actual condition. In fact, the void fraction estimated according to the homogeneous model corresponds the highest possible value for upward flow; hence, it is expected that the gravitational pressure drop parcel is slightly higher than the estimated, and $\Delta p_f$ is smaller than the estimated value.

Alternative void fraction predictive methods were also evaluated. Figure 8 depicts the $\Delta p_{total}$ and $\Delta p_f$ determined based on distinct void fraction predictive methods available in the open literature for horizontal and vertical upward flows. According to this figure, it can be noticed that the estimated void fraction value has significant impact on the determination of the frictional pressure drop parcel, and for the case of void fraction evaluated according to Turner and Wallis (1965) method, even negative frictional pressure drop values are obtained. Therefore, based on the analysis of the laser emitter and sensor system, it can be concluded that the void fraction value is considerably high, and the adoption of complex predictive methods would not be reasonable since they do not necessarily provide higher accuracy when compared with the homogeneous model.

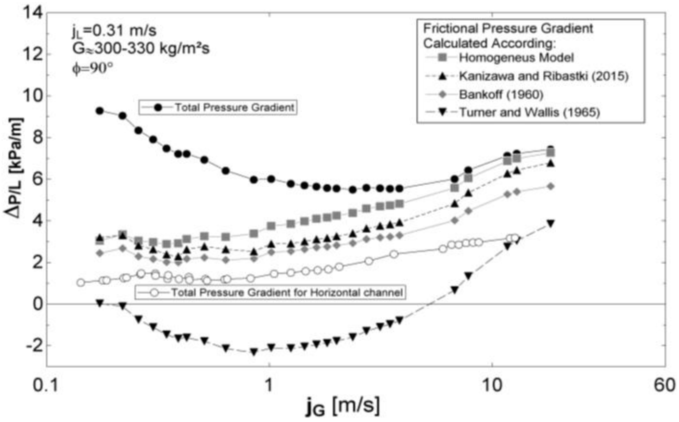


Figure 8. Variation of $\Delta p_{total} / L$ and $\Delta p_f / L$ with $j_G$ according to different void fraction models for $\phi=90°$ compared with the pressure gradient for horizontal channel.

Such a result is incorrect and corroborates the aspect related to the fact that care should be exercised when using to predict the total pressure drop in inclined flows void fraction and frictional pressure drop prediction methods whose developments were realized independently.

## 4. CONCLUSIONS

In the present study, more than 2,000 experimental data points were obtained for gas-liquid flow inside a rectangular channel (6.0 x 6.5 mm$^2$) for inclination angles ranging from -90º to +90° and mass velocities between 90 and 760 kg/m²s. Flow patterns were identified according subjective and objective approaches and pressure drop were measured. Based on this broad database, the following main conclusions can be drawn:

- The flow pattern transitions characterized according to the k-means method and based on visual evaluation of flow pattern images are similar;
- The variations of two-phase flow characteristics with varying the inclination angle from horizontal to upward flows are not significantly pronounced. On the other hand, vertical and inclined downward flows present significant differences when compared with horizontal and upward flows, which is mainly related to the gravitational forces that promotes higher liquid velocity for downward flows.
- The pressure drop is affected by the flow pattern transition, especially in the region of the flow pattern map corresponding to the transition between bubbles and intermittent flow pattern. Therefore, it can be concluded that the channels inclination also impacts the pressure drop tendencies due to the variation of flow pattern transitions with channel inclination. It can be also highlighted that the gravitational pressure drop parcel corresponds to a significant parcel of the total pressure drop for inclined and vertical, upward and downward flow.
- It is still not clear which void fraction predictive method is capable of correctly representing the actual condition, which also impacts in the estimative of gravitational and frictional pressure drop parcels.

## 5. ACKNOWLEDGEMENTS

The authors gratefully acknowledge CNPq (The National Council for Scientific and Technological Development, Brazil) for the financial support under Contract Numbers nº 476763/2013-4 and 303852/2013-5, and CONICYT (The National Commission for Scientific and Technological Research, Chile) for the scholarship granted for the first author under Contract Number 7314089, and to FAPESP (São Paulo Research Foundation) for the scholarship granted for the second author under contract number 2010/06902-9. The technical support given to this investigation by Mr. José Roberto Bogni is also appreciated and deeply recognized.

## 6. REFERENCES


Barnea, D., and Taitel, Y., (1986). Flow pattern transition in two-phase gas-liquid flows. Encyclopedia of fluid mechanics, Vol. 3, p. 403-474.

Bankoff, S. G. (1960). A Variable Density Single Fluid Model Two-Phase Flow with Particular Reference to Steam-Water. *J. Heat Transfer*, Vol 11, p. 265-272.

Chen, Y., Chen, Y. M., Yang, B. C., & Wang, C. C., (2009). Two-phase flow pattern and frictional performance across small rectangular channels. *Applied Thermal Engineering*, Vol. 29, n. 7, p. 1309-1318.

Cheng, L., Ribatski, G., & Thome, J. R. (2008). Two-phase flow patterns and flow-pattern maps: fundamentals and applications. *Applied Mechanics Reviews*, Vol 61, n. 5, p. 050802.

Coleman, J. W., and Garimella, S., (1999). Characterization of two-phase flow patterns in small diameter round and rectangular tubes. *International Journal of Heat and Mass Transfer*, Vol. 42, n. 15, p. 2869-2881.

Coleman, J. W., and Garimella, S., (2003). Two-phase flow regimes in round, square and rectangular tubes during condensation of refrigerant R134a. *International Journal of Refrigeration*, Vol. 26, n. 1, p. 117-128.

Do Nascimento, F. J., and Ribatski, G., (2010). Análise da literatura sobre dissipadores de calor baseados em multi-microcanais. In *Proceedings 4th National Congress of Mechanical Engineering*, *Campina Grande, Brazil*.

Ide, H., Kariyasaki, A., and Fukano, T., (2007). Fundamental data on the gas–liquid two-phase flow in minichannels. *International Journal of Thermal Sciences*, Vol. 46, n. 6, p. 519-530.

Kanizawa, F. T., and Ribatski, G. (2016). Void fraction predictive method based on the minimum kinetic energy. *Journal of the Brazilian Society of Mechanical Sciences and Engineering*, vol. 38, n. 1, p. 209-225.

Kew, P. A., & Cornwell, K. (1997). Correlations for the prediction of boiling heat transfer in small-diameter channels. *Applied Thermal Engineering*, Vol. 17, n. 8, p. 705-715.Kew, P. A., & Cornwell, K. (1997). Correlations for the prediction of boiling heat transfer in small-diameter channels. Applied Thermal Engineering, 17(8), 705-715.

Kim, S. M., and Mudawar, I., (2014). Review of databases and predictive methods for pressure drop in adiabatic, condensing and boiling mini/micro-channel flows. *International Journal of Heat and Mass Transfer*, Vol. 77, p. 74-97.

Lee, H. J., and Lee, S. Y., (2001). Pressure drop correlations for two-phase flow within horizontal rectangular channels with small heights. *International Journal of Multiphase Flow*, Vol. 27, n. 5, p. 783-796.

Mishima, K., Hibiki, T., and Nishihara, H., (1993). Some characteristics of gas-liquid flow in narrow rectangular ducts. *International Journal of Multiphase Flow*, Vol. 19, n. 1, p. 115-124.

Mishima, K., and Hibiki, T., (1996). Some characteristics of air-water two-phase flow in small diameter vertical tubes. *International Journal of Multiphase Flow*, Vol. 22, n. 4, p. 703-712.

Ribatski, G., Navarro, H. A., Cabezas-Gómez, L., & Saíz-Jabardo, J. M., (2007). The advantages of evaporation in micro-scale channels to cool microelectronic devices. *Thermal Engineering*, Vol. 6, n. 2, p. 34-39.

Sempertegui-Tapia, D., De Oliveira Alves, J., & Ribatski, G., (2013). Two-phase flow characteristics during convective boiling of halocarbon refrigerants inside horizontal small-diameter tubes. *Heat Transfer Engineering*, Vol. 34, n. 13, p. 1073-1087.

Shah, R. K., and London, A. L., (1978). Laminar Flow Forced Convection in Duts: A Source Book for Compact Heat Exchanger Analytical Data. Academic press.

Su, T., and Dy, J., (2004). A deterministic method for initializing k-means clustering. In Tools with Artificial Intelligence. *ICTAI 2004. 16th IEEE International Conference*, p. 784-786.

Turner, J. M., and Wallis, G. B., (1965). The separate-cylinders model of two-phase flow. Paper no. NYO-3114-6 Thayer's School Eng., Dartmouth College, Hanover, NH, USA.

Wambsganss, M. W., Jendrzejczyk, J. A., France, D. M., and Obot, N. T., (1992). Frictional pressure gradients in two-phase flow in a small horizontal rectangular channel. *Experimental Thermal and Fluid Science*, Vol. 5, n. 1, p. 40-56.

Wölk, G., Dreyer, M., and Rath, H. J., (2000). Flow patterns in small diameter vertical non-circular channels. *International journal of multiphase flow*, Vol. 26, n. 6, p. 1037-1061.

Zhao, J., Liu, G., and Li, B. (2004). Two-phase flow patterns in a square mini-channel. *Journal of Thermal Science*, Vol. 13, n. 2, p. 174-178.


## 7. RESPONSIBILITY NOTICE

The authors are the only responsible for the printed material included in this paper.